Influence of amino acid residue 374 of cytochrome *P*-450 2D6 (CYP2D6) on the regio- and enantio-selective metabolism of metoprolol

S. Wynne ELLIS*†, Karen ROWLAND*, Mark J. ACKLAND‡, Eleni REKKA§, Anthony P. SIMULA‖, Martin S. LENNARD*, C. Roland WOLF‖ and Geoffrey T. TUCKER*

*University of Sheffield, Department of Medicine and Pharmacology, Royal Hallamshire Hospital, Sheffield S10 2JF, U.K., ‡Upjohn Laboratories-Europe, Fleming Way, Crawley RH10 2LZ, U.K., §Department of Pharmaceutical Chemistry, University of Thessaloniki, 540 06 Thessaloniki, Greece, and ‖Biomedical Research Centre, Ninewells Hospital and Medical School, Dundee DD1 9SY, U.K.

Cytochrome *P*-450 2D6 (CYP2D6) is an important human drug-metabolizing enzyme responsible for the oxidation of more than 30 widely used therapeutic agents. The enzymes encoded by the published genomic [Kimura, Umeno, Skoda, Meyer and Gonzalez (1989) Am. J. Hum. Genet. **45**, 889–904] and cDNA [Gonzalez, Skoda, Kimura, Umeno, Zanger, Nebert, Gelboin, Hardwick and Meyer (1988) Nature **331**, 442–446] sequences of *CYP2D6*, and presumed to represent wild-type sequences, differ at residue 374 and encode valine (CYP2D6-Val) and methionine (CYP2D6-Met) respectively. The influence of this amino acid difference on cytochrome *P*-450 expression, ligand binding, catalysis and stereoselective oxidation of metoprolol was investigated by the heterologous expression of the corresponding cDNAs in the yeast *Saccharomyces cerevisiae*. The level of expression of apo- and holo-protein was similar with each form of *CYP2D6* cDNA, and the binding affinities of a series of ligands to CYP2D6-Val and CYP2D6-Met were identical. The enantioselective O-demethylation and α-hydroxylation of metoprolol were also similar with each form of CYP2D6, O-demethylation being *R*-(+)- enantioselective (CYP2D6-Val: *R*/*S*, 1.6; CYP2D6-Met: *R*/*S*, 1.4), whereas α-hydroxylation showed a preference for *S*-(−)-metoprolol (CYP2D6-Val: *R*/*S*, 0.7; CYP2D6-Met: *R*/*S*, 0.8). However, although the favoured regiomer overall was *O*-demethylmetoprolol (ODM), the regioselectivity for O-demethylation of each metoprolol enantiomer was significantly greater for CYP2D6-Val [*R*-(+)-: ODM/α-hydroxymetoprolol (αOH), 5.9; *S*-(−)-: ODM/αOH, 2.5) than that observed for CYP2D6-Met [*R*-(+)-: ODM/αOH, 2.2; *S*-(−)-: ODM/αOH, 1.4]. The stereoselective properties of CYP2D6-Val were consistent with those observed for CYP2D6 in human liver microsomes. The difference in the stereoselective properties of CYP2D6-Val and CYP2D6-Met were rationalized with respect to a homology model of the active site of CYP2D6 based on an alignment with the crystal structure of the bacterial cytochrome *P*-450$_{BM-3}$, CYP102.

INTRODUCTION

Cytochrome *P*-450 2D6 (CYP2D6), also known as debrisoquine 4-hydroxylase, is an important human drug-metabolizing enzyme. It is responsible for the metabolism of many therapeutic agents, including cardiac antiarrhythmics, β-adrenergic antagonists, antidepressants and neuroleptics [1,2], and some drugs of abuse, such as ecstasy [3]. An additional significant feature of CYP2D6 is its marked genetic polymorphism, often referred to as the debrisoquine/sparteine polymorphism [4–6]. This polymorphism is inherited as an autosomal recessive trait and is due to mutant or null alleles resulting in absent or functionally deficient CYP2D6 protein [7–11].

The published cDNA [12] and genomic [13] sequences of *CYP2D6*, presumed to represent wild-type sequences, encode identical proteins except for a single amino acid difference at position 374, namely methionine in the cDNA sequence and valine in the genomic sequence. Independently, we have isolated a cDNA of *CYP2D6* and found that the encoded amino acid sequence was identical to that of the genomic sequence, encoding valine at position 374 [14,15].

Multiple alignment studies of the CYP2 family relative to cytochrome *P*-450$_{cam}$ from *Pseudomonas putida* (CYP101) [16–18] indicate that amino acid residue 374 lies in the conserved β1–4 sheet region of CYP2D6. It is located in one of the six (fifth) substrate recognition sites (SRSs) inferred by Gotoh [16] as being important in substrate binding in the CYP2 family of cytochrome *P*-450s. A recent multiple alignment study [19] based on structural comparisons between the crystal structures of three bacterial cytochrome *P*-450s, namely CYP101 [20], cytochrome *P*-450$_{BM-3}$ from *Bacillus megaterium* (CYP102) [21] and cytochrome *P*-450$_{terp}$ from *Pseudomonas* sp. (CYP108) [22], supports the SRS designations of Gotoh [16] but stipulates minor changes to the alignments at SRS2 and SRS4. Together, these data suggest that amino acid residue 374 lies in the active site of CYP2D6 and could influence substrate specificity and/or catalytic activity.

Homology models of the active site of CYP2D6 have been generated [18,23] based on alignments with the structures of CYP101 and CYP102 respectively. However, these models did not identify amino acid 374 as a possible residue in the active site of CYP2D6. We have investigated the influence of Val-374 and Met-374 on the catalytic activity of CYP2D6 by the heterologous

Abbreviations used: CYP2D6, cytochrome *P*-450 2D6; CYP2D6-Val, cytochrome *P*-450 2D6 containing valine at amino acid position 374; CYP2D6-Met, cytochrome *P*-450 2D6 containing methionine at amino acid position 374; CYP101, cytochrome *P*-450$_{cam}$ from *Pseudomonas putida*; CYP102, cytochrome *P*-450$_{BM-3}$ from *Bacillus megaterium*; CYP108, cytochrome *P*-450$_{terp}$ from *Pseudomonas* sp.; SRS, substrate recognition site; ODM, *O*-demethylmetoprolol; αOH, α-hydroxymetoprolol.

† To whom correspondence should be addressed.

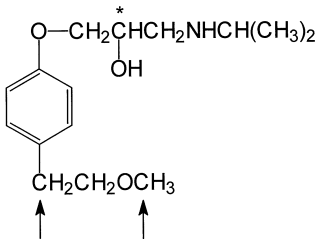

Figure 1 Structure of metoprolol showing sites of oxidation (↑) and chiral centre (*)

expression of the two isolated *CYP2D6* cDNAs in the yeast *Saccharomyces cerevisiae* [14]. Using metoprolol (Figure 1) as a probe substrate [24], the regio- and enantio-selective properties of microsomal preparations of yeast-derived CYP2D6-Val and CYP2D6-Met were compared with that of native CYP2D6 in microsomes isolated from four human livers. The experimental data were subsequently related to a computer-derived homology model of the active site of CYP2D6 based on alignment with the crystal structure of CYP102.

EXPERIMENTAL

Materials

CYP2D6 cDNAs were isolated by Dr. F.J. Gonzalez [12] and by us (C.R. Wolf, unpublished work). DNA-modifying enzymes were purchased from Northumbria Biologicals Limited (Cramlington, U.K.). Linker DNA (*Bam*HI 8-mer) was purchased from Promega (Madison, WI, U.S.A.). Geneclean for DNA purification was purchased from BIO 101 (La Jolla, CA, U.S.A.). The yeast expression vector, pMA91, carrying the phosphoglycerate kinase promoter and terminator, was a gift from Dr. S. Kingsman (Oxford University, Oxford, U.K.). *Escherichia coli* DH5α (F^- *recA*1 *endA*1 *gyrA*96 *thi*-1 *hsdR*17 *relA*1 *suppE*44 λ-Δ*lacU*169 080*lacZ* ΔM15) and *S. cerevisiae* AH22 strain (ρ° a *leu*2-3 *leu*2-112 *can*1 *cir*$^+$ *his*4-519) were used as host strains. Yeast nitrogen base without amino acids, bacto-peptone, bacto-tryptone and bacto-agar were purchased from Difco Laboratories (Detroit, MI, U.S.A.). Human liver microsomes (HL5, HL7, HL9 and HL10) were prepared from livers in our liver bank [25]. Microsomes from human lymphoblastoid cells (AHH-1), transfected with and without a functional human *CYP2D6*-Met cDNA, were purchased from the Gentest Corporation (Woburn, MA, U.S.A.). Metoprolol tartrate (racemate), and *O*-demethylmetoprolol (ODM) and α-hydroxymetoprolol (αOH) hydroxybenzoate metabolites were gifts from AB Hässle (Mölndal, Sweden). The hydrochloride salts of *R*-(+)- and *S*-(−)-metoprolol were gifts from Ciba-Geigy (Basle, Switzerland). All other chemicals were purchased from Sigma (Poole, Dorset, U.K.) and were of the highest grade of purity.

Construction of expression plasmids (pELT1 and pELT2)

Recombinant DNA procedures were performed according to standard methods [26]. Briefly, the coding region of each *CYP2D6* cDNA was isolated as an *Eco*RI fragment (1.56 kb) from pTZ19R-based vectors (pMP201 and pMP102). The 3′ recessed ends were filled in with Klenow and the blunt ends modified with *Bam*HI linkers (8-mer). Following *Bam*HI digestion, each *Bam*HI-modified cDNA was ligated into the *Bgl*II cloning site of the expression plasmid pMA91 such that the ATG start codon of the *CYP2D6* gene was distanced minimally (12 bp) from the end of the phosphoglycerate kinase promoter. Correct orientation of each cDNA was then verified by restriction analysis. Sequencing of the two cDNAs and the 5′ junction region of the constructed recombinant expression plasmids, pELT1 encoding valine and pELT2 encoding methionine at residue 374, was performed by the dideoxy method using the Sequenase version 2.0 kit (Amersham International, Amersham, U.K.).

Yeast culture conditions and microsome preparation

Transformation of *S. cerevisiae* was by electroporation [27]. Yeast cells transformed with pMA91, pELT1 or pELT2 were grown in batch culture comprising 1 l of liquid synthetic medium [0.67 % (w/v) yeast minimal medium without amino acids, 0.04 % (w/v) histidine and 3 % (w/v) glucose] in 2 l flasks for 42 h (to stationary phase) on an orbital shaker (200 r.p.m.) at 30 °C. All subsequent steps were performed at 0–4 °C. Yeast cells were harvested by centrifugation, washed with ice-cold distilled water and resuspended in 20 ml of ice-cold 0.1 M potassium phosphate buffer (pH 7.4) containing 0.65 M sorbitol and 0.1 mM EDTA (microsomal buffer). Yeast cells were disrupted mechanically with glass beads (0.45–0.05 mm) at 4000 r.p.m. for 40 s with liquid carbon dioxide cooling in an MSK Cell Homogeniser (B. Braun Medical Limited, Aylesbury, U.K.). The microsomal fraction was prepared by centrifugation of the homogenate at 15000 ***g*** for 30 min at 4 °C to remove residual whole cells, cell debris and mitochondria, followed by a further centrifugation at 100000 ***g*** for 2 h at 4 °C (Beckman L-80 ultracentrifuge, Ti rotor) to sediment the microsomal (endoplasmic membrane) pellet. The pellet was washed twice with 5 ml of microsomal buffer and resuspended in the same buffer at a protein concentration of 15–30 mg/ml. Aliquots (0.5 ml) were immediately flash-frozen in liquid nitrogen and stored at −80 °C prior to use.

Human liver microsomes were prepared as described previously [28] and stored at −80 °C as a suspension in 0.1 M potassium phosphate buffer (pH 7.4) containing 30 % (v/v) glycerol.

Spectrophotometric measurements

The cytochrome *P*-450 content of yeast microsomes was measured by reduced CO difference spectroscopy using an absorbance coefficient of 91 $mM^{-1} \cdot cm^{-1}$, essentially according to the method of Omura and Sato [29]. Briefly, samples (1 ml) of microsomal suspension were reduced for 2 min with 20 μl of a fresh aqueous solution of $Na_2S_2O_4$ (100 mg/ml). A baseline of equal absorbance was recorded using a Shimadzu UV/Vis-3000 double-beam dual-wavelength spectrophotometer. CO was bubbled through the contents of the sample cuvette for 1 min, and the resulting difference spectrum was recorded 6 min after the initial addition of $Na_2S_2O_4$.

Apparent dissociation constants (K_s) of several known ligands of CYP2D6 were determined from substrate-induced difference spectra [30]. Briefly, a baseline of equal absorbance of yeast microsomes containing 0.1–0.5 μM CYP2D6 was recorded from 500 to 350 nm using a Shimadzu UV/Vis-3000 spectrophotometer. Difference spectra were then recorded every two min after incremental additions of ligand (usually dissolved in dimethyl sulphoxide) to the sample cuvette and the equivalent volume of solvent to the reference cuvette. The final dilution was less than 2 %. Apparent K_s values were determined from double reciprocal plots of absorbance change (ΔA 385–420 nm) against substrate concentration.

Microsomal incubations

Incubations at a single substrate concentration were conducted in glass tubes with 10 pmol of yeast-derived CYP2D6-Val, CYP2D6-Met or lymphoblastoid-derived CYP2D6-Met (0.1–0.3 mg of microsomal protein), 40 μM *R*-(+)-, *S*-(−)- or racemic metoprolol dissolved in 1.15% (w/v) KCl and a NADPH-generating system dissolved in 0.2 M potassium phosphate buffer (pH 7.4). The NADPH-generating system consisted of 0.4 μmol of NADP, 4 μmol of glucose 6-phosphate, 2 μmol of $MgCl_2$, and 0.4 unit of glucose-6-phosphate dehydrogenase. The total incubation volume was 0.5 ml. All reactions were initiated by the addition of microsomes, and incubations were carried out at 37 °C for 10 min under open air in a shaking water bath (100 oscillations/min). The metabolic reactions were terminated by transferring 0.45 ml of incubate to plastic vials containing 50 μl of 6% (v/v) perchloric acid. Preliminary experiments indicated that the formation velocities of metabolites of each substrate were linear up to 10 min and 2 mg of microsomal protein.

Kinetic analyses of the O-demethylation and α-hydroxylation of metoprolol enantiomers by yeast and human liver microsomes were made over a substrate concentration range of 5–2000 μM. Four different microsomal preparations of yeast-derived CYP2D6-Val and CYP2D6-Met were investigated together with microsomes prepared from four different human livers (HL5, HL7, HL9 and HL10). Incubations of each microsomal preparation were performed in duplicate at each substrate concentration. As controls, boiled human microsomes and microsomes prepared from yeast cells transformed with plasmid lacking *CYP2D6* cDNA were included in each set of incubations.

Analysis of metoprolol metabolites

Metabolites were assayed according to a modification of the method of Otton and co-workers [24]. An internal standard, guanoxan hemisulphate (2 μg), was added to each inactivated incubation mixture and vortexed before centrifugation at 12000 ***g*** to precipitate the microsomal protein. Aliquots (0.45 ml) of supernatant were transferred to glass tubes containing 0.5 ml of 4 M NaOH and 5 ml of methyl-*tert*-butyl ether, and the mixture was vortexed at room temperature for 2 min. After centrifugation at 900 ***g*** for 5 min, the organic phase was transferred to conical glass tubes and evaporated to dryness under vacuum at 40 °C using a Buchler vortex–evaporator (Baired and Tatlock, Romford, U.K.). The residue was reconstituted in 200 μl of mobile phase comprising water/acetonitrile (90:10, v/v) containing 1% (w/v) triethylamine adjusted to pH 3 with orthophosphoric acid and subjected to HPLC analysis. The sample was applied to a Z-module column system containing a Nova-Pak C18 reverse-phase cartridge (Millipore, Harrow, U.K.) and eluted with the mobile phase at a flow rate of 3.0 ml/min. The eluate was monitored with a 970FS Schoeffel/Kratos fluorescence detector (HPLC Technology, Macclesfield, U.K.) operated at an excitation wavelength of 193 nm and with an emission filter at 300 nm.

Calibration samples were prepared by adding the appropriate concentrations of ODM and αOH to 0.5 ml of yeast microsomes, prepared from cells transformed with plasmid pMA91, in 0.2 M potassium phosphate buffer (pH 7.4). The concentration range of standards was 0.05–0.4 μM for ODM and 0.045–0.35 μM for αOH. After adding an internal standard (guanoxon hemisulphate; 2 μg), the calibration samples were processed in the same manner as described for the incubation samples. The peak height ratios of metabolites versus that of the internal standard were plotted against the standard concentrations.

The limit of detection of ODM and αOH was 15 nM. The coefficients of variation for the assay were less than 5% at ODM and αOH concentrations of 0.8 and 0.7 μM respectively.

Data analysis

Data from kinetic experiments were analysed by NONLIN, an iterative least-squares fitting program, using initial estimates of K_m and V_{max} obtained from Eadie–Hofstee plots. The kinetic parameters were compared by analysis of variance. When significant differences were noted between groups, the data were compared using the Mann–Whitney test.

Computational methods

Molecular modelling was performed using the in-house Upjohn modelling system known as 'MOSAIC'. Crystal co-ordinates of CYP102 were taken from the Brookhaven Protein Databank (code 2HPD) [31] to use as a core framework for modelling. The active site and channel regions comprising the haem group and residues Thr-10–Val-26, Phe-42–Tyr-51, Asn-70–Ser-89, Ser-176–Asp-194, Ile-259–Thr-269, Pro-326–Leu-333, Glu-352–Ile-357 and Glu-435–Lys-439 of CYP102 [21] were extracted from the X-ray crystal structure and the residues substituted with those of CYP2D6 according to the alignment in Figure 3 [18]. Energy minimization was performed using the Macromodel/Batchmin version 3.5 implementation of Amber [32]. The protein backbone and haem moiety were fixed during energy minimization in order to prevent excessive displacement of the secondary structural elements. The CYP2D6 probe substrate metoprolol was docked visually into the active site, the aromatic ring being positioned in a perpendicular fashion with respect to the haem moiety [33]. The basic nitrogen of the substrate, which is thought to interact with a negatively charged binding site in the protein [34], was positioned 2.5–4.5 Å [33] from the carboxylate anion of aspartic acid-301, the amino acid implicated [23,33], and recently confirmed [35], as the residue involved in this specific electrostatic interaction. Each site of oxidation of metoprolol (methoxy carbon and α-methylene carbon) was positioned 4 Å [20,33] from the catalytic iron atom of the haem moiety. These positional constraints conform with the published pharmacophore models of CYP2D6 substrates, which specify a distance of 5 or 7 Å [34,36,37] from the site of oxidation to the basic nitrogen atom of the substrate. This procedure was used to dock *R*-(+)- and *S*-(−)-metoprolol in the active site of CYP2D6 encoding either valine or methionine at position 374. Following the adoption of these constraints, energy minimization was performed as indicated previously.

RESULTS

Spectral characterization

The reduced CO-difference spectra of microsomes prepared from yeast cells expressing CYP2D6-Val and CYP2D6-Met showed similar specific contents of holo-protein (37 ± 36 and 40 ± 33 pmol·mg^{-1} microsomal protein respectively), both with Soret peaks at 448 nm and no detectable cytochrome *P*-420 (Figure 2). Furthermore, immunoblot analysis revealed similar levels of apo-protein in each microsomal preparation (results not shown).

Substrate-induced difference spectra with yeast-derived CYP2D6-Val and CYP2D6-Met microsomal preparations illustrated identical binding properties, classical type I spectra ($\lambda_{max} \sim 385$ nm, $\lambda_{min} \sim 420$ nm) being obtained with all tested substrates and inhibitors, including quinidine, a selective potent inhibitor of CYP2D6 [24]. The apparent K_s values of each ligand

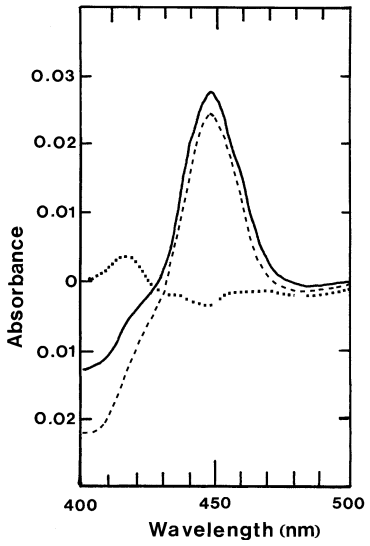

Figure 2 Reduced CO difference spectra of microsomes prepared from yeast cells transformed with *CYP2D6*-Val (– –) and *CYP2D6*-Met (—)

Control (· · ·) microsomes were prepared from yeast cells transformed with plasmid lacking *CYP2D6* cDNA. Microsomal protein content was 5 mg/ml.

Table 1 Type I binding coefficients (K_s) of known ligands of CYP2D6 determined with microsomes prepared from yeast expressing CYP2D6-Val and CYP2D6-Met

Values are means of two determinations.

Ligand	Apparent binding coefficients (μM)	
	CYP2D6-Val	CYP2D6-Met
R-(+)-metoprolol	28.3	26.5
S-(−)-metoprolol	9.2	10.6
Debrisoquine	8.9	9.1
Sparteine	9.3	9.6
SKF-525A	8.8	9.6
Moclobemide	2.0	2.5
Quinidine	0.1	0.1

were similar with both forms of CYP2D6 (Table 1), quinidine having 100-fold greater affinity than the CYP2D6 probe substrates metoprolol, debrisoquine and sparteine.

Formation of ODM and αOH from *R*-(+)- and *S*-(−)-metoprolol

Estimates of the apparent Michaelis–Menten constants for O-demethylation and α-hydroxylation of *R*-(+)- and *S*-(−)-metoprolol with yeast-derived CYP2D6-Val and CYP2D6-Met are shown in Table 2. The K_m values for both oxidative processes were in the low micromolar range, between 17 and 46 μM. No significant difference was detected between the affinity of CYP2D6-Val for O-demethylation and α-hydroxylation of *R*-(+)- and *S*-(−)-metoprolol. The affinity of CYP2D6-Met for O-demethylation and α-hydroxylation of *S*-(−)-metoprolol was similar to that observed with CYP2D6-Val, although the K_m values for both routes of oxidation of *R*-(+)-metoprolol were marginally, yet significantly, lower than those of *S*-(−)-metoprolol (19 and 17 μM; $P < 0.05$) (Table 2).

With both CYP2D6-Val and CYP2D6-Met, the V_{max} values for O-demethylation of *R*-(+)- and *S*-(−)-metoprolol were consistently higher than the corresponding α-hydroxylation values. However, significant differences in the regioselective metabolism of the two forms of CYP2D6, as measured by the ratio of O-demethylation to α-hydroxylation of each enantiomer, were observed (Table 2). Thus with *R*-(+)-metoprolol an ODM/αOH ratio of 5.9 was obtained with CYP2D6-Val, in contrast to an ODM/αOH ratio of 2.2 with CYP2D6-Met. Smaller, but still significant, differences in regioselectivity between the two forms of CYP2D6 were observed with *S*-(−)-metoprolol (Table 2). These differences in regioselectivity were a consequence of decreases (30–40 %) in the rate of O-demethylation and increases (30–60 %) in the rate of α-hydroxylation with CYP2D6-Met relative to CYP2D6-Val. The regioselective differences between CYP2D6-Val and CYP2D6-Met were also apparent when racemic metoprolol at a single substrate concentration (40 μM) was incubated with the two forms of CYP2D6. Thus with the racemate, ODM/αOH ratios of 3.8:1 (ODM, 1.88; αOH, 0.50 pmol/min per pmol of cytochrome *P*-450) and 1.9:1 (ODM, 1.28; αOH, 0.68 pmol/min per pmol of cytochrome *P*-450) were observed with CYP2D6-Val and CYP2D6-Met respectively. These ratios are similar to the ODM/αOH ratios interpolated from the combined *R*-(+) and *S*-(−) enantiomer data shown in Table 2 (CYP2D6-Val, 4.2; CYP2D6-Met, 1.8) indicating mutual competition between the enantiomers in the racemic mixture.

In contrast to the significant differences in the regioselectivity

Table 2 Estimates of the apparent Michaelis–Menten constants for the O-demethylation and α-hydroxylation of *R*-(+)- and *S*-(−)-metoprolol by yeast-derived CYP2D6-Val and CYP2D6-Met, and human liver CYP2D6

CYP2D6-Val and CYP2D6-Met data are means ± S.D. of four experiments. Human liver data are means ± S.D. from four different CYP2D6 extensive metabolizer livers, each conducted in duplicate. V_{max} values are expressed as pmol of product/min per pmol of cytochrome *P*-450 for yeast-derived data, and pmol of product/min per mg of microsomal protein for human liver data.

	R-(+)-Metoprolol				*S*-(−)-Metoprolol				Regioselectivity ODM/αOH (V_{max} ratio)		Enantioselectivity *R*-(+)/*S*-(−) (V_{max} ratio)	
	ODM		αOH		ODM		αOH					
	K_m (μM)	V_{max}	K_m (μM)	V_{max}	K_m (μM)	V_{max}	K_m (μM)	V_{max}	*R*-(+)	*S*-(−)	ODM	αOH
CYP2D6-Val	46 ± 19	4.39 ± 0.44	31 ± 4	0.75 ± 0.07	46 ± 8	2.71 ± 0.12	42 ± 14	1.12 ± 0.09	5.9 ± 1.1	2.5 ± 0.2	1.6 ± 0.2	0.7 ± 0.1
CYP2D6-Met	19 ± 10	2.65 ± 0.17	17 ± 7	1.21 ± 0.12	34 ± 6	1.89 ± 0.16	33 ± 8	1.45 ± 0.06	2.2 ± 0.1	1.4 ± 0.1	1.4 ± 0.1	0.8 ± 0.1
Human liver CYP2D6	29 ± 9	177 ± 44	44 ± 17	45 ± 14	36 ± 19	104 ± 23	38 ± 22	51 ± 15	4.0 ± 0.5	2.1 ± 0.4	1.7 ± 0.1	0.9 ± 0.1

Table 3 Comparison of the O-demethylation and α-hydroxylation of *R*-(+)- and *S*-(−)-metoprolol (40 μM) by yeast- and human lymphoblastoid-derived CYP2D6-Met

Values are means ± S.D. of four experiments.

	Yeast-derived CYP2D6-Met			Lymphoblastoid-derived CYP2D6-Met		
	ODM	αOH		ODM	αOH	
Enantiomer	pmol/min per pmol of cytochrome *P*-450		Regioselectivity (ODM/αOH ratio)	pmol/min per pmol of cytochrome *P*-450		Regioselectivity (ODM/αOH ratio)
R-(+)-Metoprolol	2.02 ± 0.31	0.79 ± 0.16	2.63 ± 0.42	1.87 ± 0.30	0.82 ± 0.11	2.30 ± 0.34
S-(−)-Metoprolol	1.13 ± 0.17	0.87 ± 0.16	1.33 ± 0.23	1.28 ± 0.15	0.90 ± 0.10	1.44 ± 0.13
Enantioselectivity *R*-(+)/*S*-(−) ratio	1.7 ± 0.2	0.9 ± 0.3		1.5 ± 0.3	0.9 ± 0.2	

of the two forms of CYP2D6, no differences in enantioselectivity were observed. Thus although O-demethylation of metoprolol was significantly *R*-enantioselective and α-hydroxylation showed a slight preference for *S*-(−)-metoprolol, this enantioselectivity was apparent with both CYP2D6-Val and CYP2D6-Met (Table 2).

Since CYP2D6-Met was available commercially in microsomes prepared from human lymphoblastoid cells (Gentest, Woburn, MA, U.S.A.), the regioselective and enantioselective properties of this cDNA-derived CYP2D6-Met were investigated using metoprolol at a single substrate concentration (40 μM). The regioselective and enantioselective properties of lymphoblastoid-derived CYP2D6-Met were similar to those observed with yeast-derived CYP2D6-Met (Table 3).

The kinetics of formation of ODM and αOH by native CYP2D6 in human liver microsomes are summarized in Table 2. The mean K_m values for both oxidative processes with each metoprolol enantiomer were not significantly different and were in the low micromolar range (between 29 and 44 μM), similar to the values obtained with yeast-derived CYP2D6 (Table 2). The V_{max} values for O-demethylation as compared with α-hydroxylation were consistently higher for both metoprolol enantiomers in all four human liver microsome preparations. This is reflected in the regioselectivity data, mean ODM/αOH ratios of 4.0 and 2.1 being observed for *R*-(+)- and *S*-(−)-metoprolol respectively (Table 2). Furthermore, V_{max} values for O-demethylation were consistently higher for *R*-(+)-metoprolol than for *S*-(−)-metoprolol. In contrast, V_{max} values for α-hydroxylation were slightly less for *R*-(+)-metoprolol compared with those for *S*-(−)-metoprolol. This is reflected in mean enantioselectivity ratios of 1.7 and 0.9 for O-demethylation and α-hydroxylation respectively (Table 2).

Homology modelling of the active site of CYP2D6

Hasemann and co-workers [19] have made a detailed comparison of three [20–22] of the four available bacterial cytochrome *P*-450 crystal structures and conclude that they are similar with respect to their overall fold and secondary structural elements. These workers also propose that, in light of their studies, all cytochrome *P*-450s will be found to possess the same tertiary structure. This claim is substantiated by the recent publication of the crystal structure of a fourth bacterial cytochrome *P*-450, cytochrome *P*-450eryf [38].

CYP102 was chosen as a template for modelling in the present study because it segregates with the eukaryotic families 4 and 52 in the cytochrome *P*-450 phylogenetic tree [21], and has only

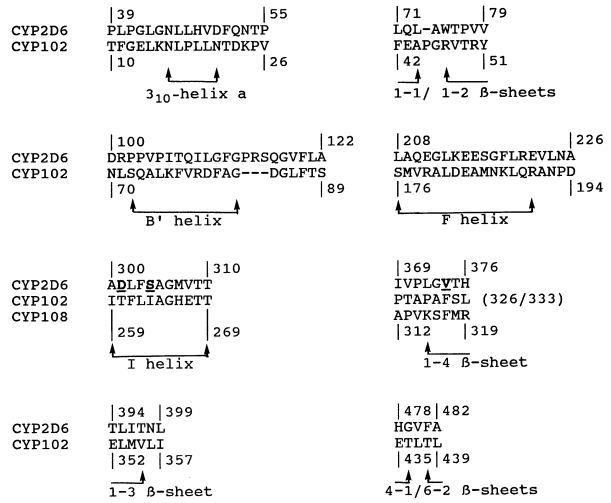

Figure 3 Alignment of the active site and channel regions of CYP2D6-Val, CYP102 and CYP108 (β1-4 region only)

The positions of the anionic binding site Asp-301 and the hydrogen bonding site Ser-304, suggested to be involved in chiral selectivity, are underlined. The Val/Met-374 locus (underlined) lies two residues from His-376, the residue responsible for binding one of the propionic acid groups of the porphyrin ring. The secondary structure regions of CYP102 are indicated [22].

marginal primary structural homology with cytochrome *P*-450s from other bacteria. Also, alignments can be generated that have fewer sequence gaps, thus removing some of the uncertainty associated with gaps in models based on CYP101. In relation to the active-site regions, it is apparent from the work of Hasemann and co-workers [19] that the location of the I helix and the β1-1, β1-2, β1-3, β1-4 and β6-2 sheet regions are similar in CYP101, CYP102 and CYP108, but that there is greater positional variation in the A, B′ and F helices and the β4-1 sheet region. Therefore a CYP2D6 active site model based on CYP102 is likely to be speculative with respect to the upper (A and F helices, β4-1 sheet) regions of the model as well as one of the active-site faces (B′ helix plus associated loop region), but acceptable with respect to the active-site faces defined by the I helix, the β1-4 sheet region (the subject of this paper) and the remaining β-sheet regions. A model was therefore built to assist the localization and visualization of amino acid 374 in the secondary structural elements of

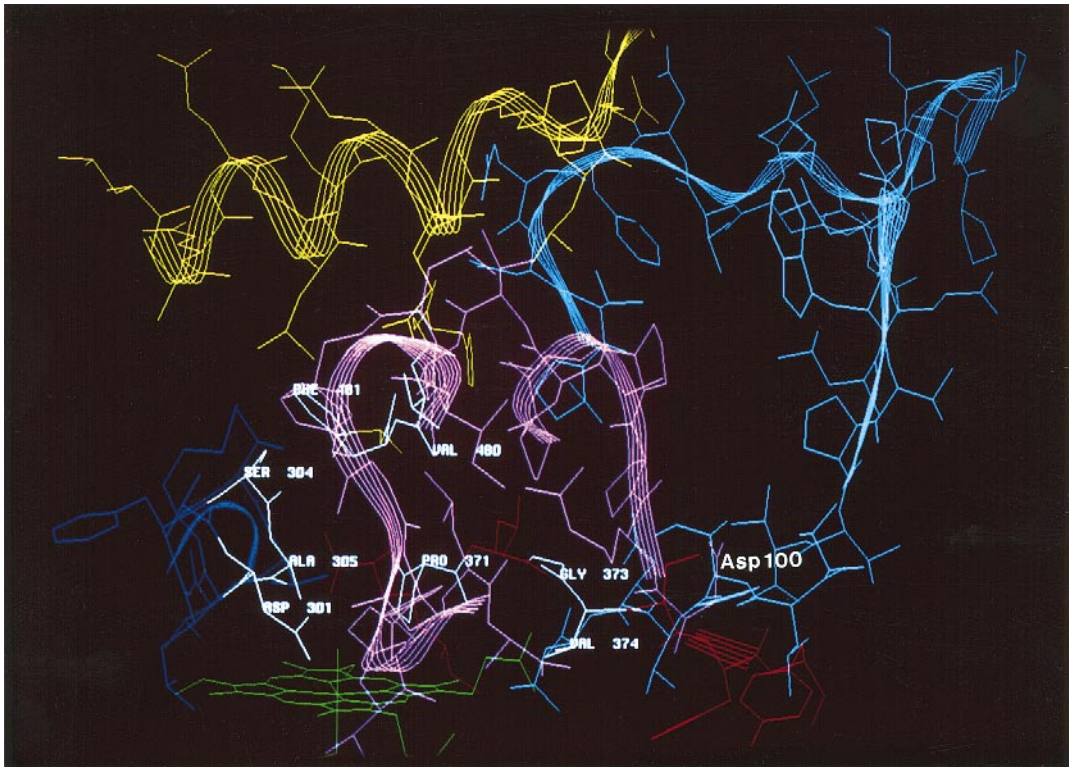

Figure 4 Active-site model generated from the alignment of CYP102 with CYP2D6-Val outlined in Figure 3

Residues are colour coded as follows: key residues including Asp-301 and Val-374 (white), Pro-39–Pro-55 and Leu-71–Val-79 (cyan), Asp-100–Ala-122 (magenta), Leu-208–Ala-226 (yellow), Ala-300–Thr-310 (blue), Ile-369–His-376 (red), Thr-394–Leu-399 (cyan), His-478–Ala-482 (yellow) and the porphyrin ring (green).

the CYP2D6 active site, relative to the probe substrate, metoprolol.

The alignment used in this study (Figure 3) is based primarily on that of Lewis [18] with a minor modification in the β1-4 region, namely movement of the sequence by one residue, such that positions Val-374 and His-376 of CYP2D6 were in alignment with Phe-331 and Leu-333 of CYP102 respectively (Figure 3). This alignment was established as a result of comparative studies between CYP102 and CYP108, which had virtually identical secondary structural elements in the β1-4 region [22]. The CYP108 sequence was useful for comparative purposes, as it possesses a basic residue (Arg-319) that is responsible for co-ordinating the haem proprionate, in common with the majority of the cytochrome *P*-450 super-family but unlike CYP102. Therefore it was possible to align His-376 (CYP2D6) with Arg-319 (CYP108) and hence Leu-333 (CYP102). It is worthy of note that the secondary structures of CYP102 and CYP108 are very similar despite having very low sequence similarity. For instance, Pro-329 (CYP102) pairs with Lys-315 (CYP108) and Pro-313 (CYP108) pairs with Thr-327 (CYP102) in different regions of the sequence, but there is no overall change in the secondary structures. This alignment is consistent with that of others [16,19,39] with respect to the I helix, which is particularly important in CYP2D6 since it forms one side of the active-site cavity. The resulting CYP2D6 active-site model is illustrated in Figure 4, and is colour coded according to sequence. The active site consists of a cavity bordered by hydrophobic residues; important active-site residues in the model include Thr-309 and Thr-312 of the oxygen-binding site, Asp-301 (anionic binding site), Ser-304 and Ala-305 of the I helix and Pro-371, Gly-373 and Val-374 of the β1-4-sheet region. The active-site area was further defined by a lipophilic pocket bordered by Val-480 and Phe-481 of the loop and β6-2 region. This model identifies Asp-301 as the critical substrate-contact residue involved in the proposed electrostatic interaction between the basic nitrogen of the substrate and a negatively charged site in the active site, which is in agreement with recent experimental data [35].

DISCUSSION

The experimental data show that the level and stability of expression of CYP2D6 is not influenced by the choice of valine or methionine at amino acid residue 374. Furthermore, this amino acid difference does not influence the substrate binding of a range of CYP2D6 ligands, as determined from their apparent binding coefficients. However, the experimental data do indicate that the choice of valine or methionine at position 374 can alter the regioselective oxidation of metoprolol but does not influence the chiral selectivity of the enzyme. The difference in regioselectivity was not a consequence of the further metabolism of ODM and αOH, since neither form of CYP2D6 was able to oxidize these primary metabolites (results not shown).

It was of interest to consider these findings with regard to the CYP2D6 active-site model. The alignment of CYP2D6 with that of CYP102 (Figure 3) clearly places residue 374 in the β1-4 sheet of the protein, which forms part of the wall of the active site. This region is well defined and can be substantiated with reference to His-376, since this residue is highly conserved throughout the cytochrome *P*-450 super-family, and is thought to be responsible for binding one of the propionic acid groups in the porphyrin

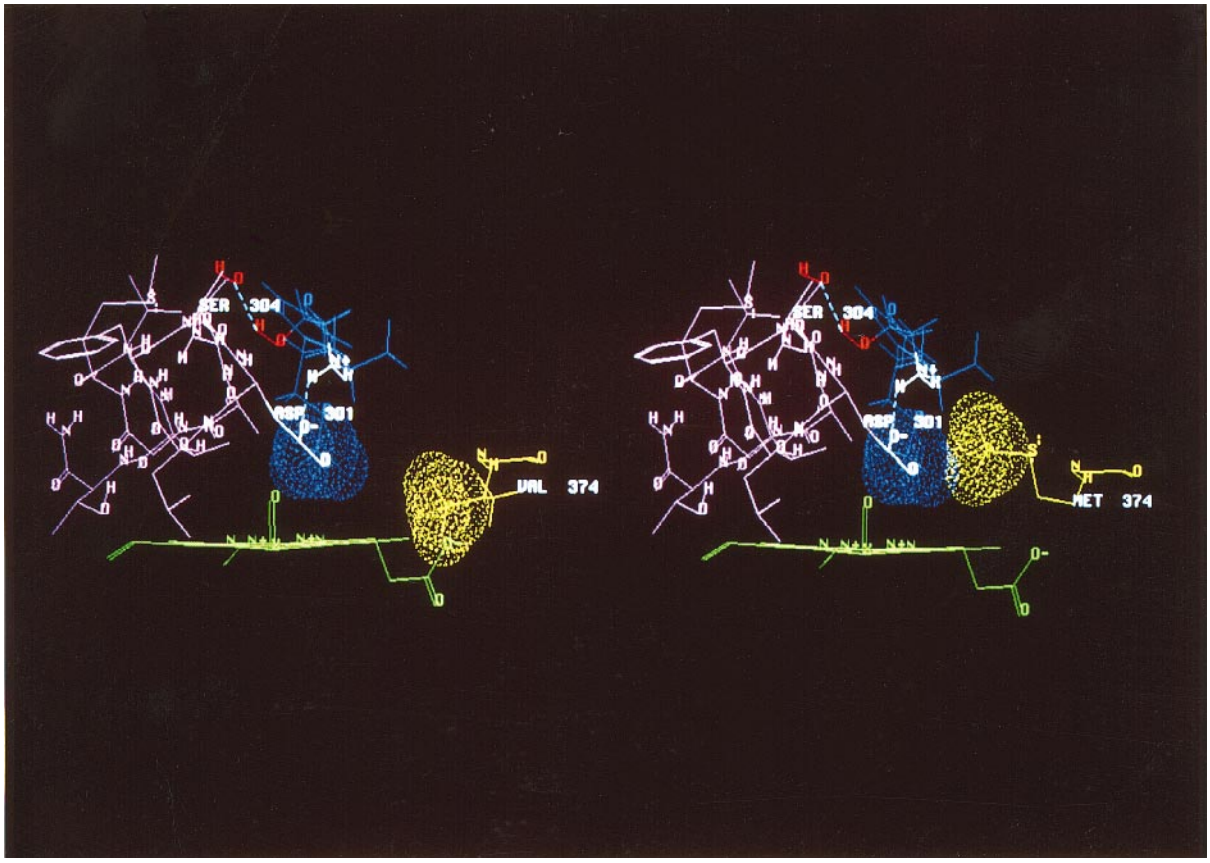

Figure 5 Features of the active site of CYP2D6-Val (left) and CYP2D6-Met (right)

Metoprolol (blue) is orientated vertically with respect to the porphyrin ring (green). The substrate makes contact with residues of the I helix (magenta) but does not interact with Val-374 (yellow) of CYP2D6-Val (left), but does contact Met-374 of CYP2D6-Met (right). Functional groups involved in electrostatic (Asp-301) and hydrogen-bonding (Ser-304) interactions are marked in white and red respectively.

ring. Modelling studies of metoprolol binding in the active site of CYP2D6-Val suggest that Val-374 (yellow in Figure 5, left-hand side) is unable to contact the substrate during the binding process and consequently is unlikely to influence the regio- or enantioselective oxidation of the substrate. However, modelling of the active site of CYP2D6-Met (yellow in Figure 5, right-hand side) indicates that Met-374, which is larger and extends into the active site, is able to contact the substrate at the catalytic centre, thereby sterically influencing the regioselective oxidation of metoprolol. It is also apparent that the Val/Met-374 locus resides on the opposite wall to, and significantly remote from, the Asp-301 and Ser-304 residues (Figures 4 and 5), both of which lie in the I helix. Residue Ser-304 lies close to, and has the potential to hydrogen bond with, the chiral alcohol of metoprolol (Figure 5), thus providing a possible explanation for the observed chiral selectivity of CYP2D6 for the metabolism of this substrate (Tables 2 and 3). Modelling studies have also shown that the chiral hydroxy group of quinidine, a potent, selective inhibitor of CYP2D6, can potentially also form a hydrogen bond with Ser-304, whereas quinine, its diastereoisomer, has less potential to undertake this interaction [18]. This could provide an explanation for the 100-fold difference in inhibition of CYP2D6 by quinidine and quinine [24]. In summary, the computational studies of the active site of CYP2D6 suggest that the Val/Met-374 locus is unlikely to influence the enantioselective properties of the enzyme but could be a determinant of regioselective metabolism. This is entirely consistent with the experimental data presented (Table 2).

As mentioned previously, a homology model of the active site of CYP2D6 requires the participation of a negatively charged residue in the protein to enable the predicted electrostatic interaction with the basic nitrogen of the substrate [34,37]. The current homology model predicts the participation of aspartic acid-301 in this interaction. This conforms with the predictions of refs. [23,33] and has been confirmed experimentally by Ellis et al. [35] by site-directed mutagenesis studies. The possible involvement of aspartic acid-100 [23] as a alternative candidate residue for this interaction cannot be rationalized with our homology model due to its peripheral location (Figure 4).

The question arises as to the nature of the discrepancy between the published cDNA and genomic sequences of *CYP2D6*. The transition of G → A at bp 1120, resulting in the change of valine to methionine at position 374 of CYP2D6, results in the loss of a unique *Mae*III (GTGAC) restriction site, thus allowing identification by restriction analysis following PCR amplification of the region of interest (244 bp spanning exon 7/intron 7). Using such an analysis, all attempts to identify individuals with *CYP2D6* sequences encoding methionine at position 374 have been unsuccessful (G. Smith and C. R. Wolf, unpublished work). Thus it would appear that the original *CYP2D6* cDNA isolated

by Gonzalez et al. [12] containing A at 1120, and encoding methionine at 374, was artifactual, possibly arising from a cloning error.

The authenticity of the two *CYP2D6* cDNAs can be further evaluated by comparison of the catalytic properties of the two cDNA-derived CYP2D6 proteins with that of native CYP2D6 in human liver microsomes. The data presented in this and previous studies [40] with human liver microsomes show that the stereoselective oxidation of metoprolol by native human CYP2D6 is more consistent with that of CYP2D6-Val than with CYP2D6-Met (Table 2), the regioselectivity of the latter being much lower than that observed with human liver CYP2D6 and CYP2D6-Val. The lower regioselectivity of CYP2D6-Met relative to human liver CYP2D6 is in agreement with data recently published by Mautz et al. [41] using human lymphoblastoid-derived CYP2D6-Met. In contrast to the difference in the regioselective oxidation of metoprolol, enantioselective metabolism by CYP2D6-Val and CYP2D6-Met was similar to that observed with native CYP2D6 in human liver microsomes. Again, this is in agreement with the data obtained using human lymphoblastoid-derived CYP2D6-Met [41].

Until recently, the only commercial source of recombinant CYP2D6 was from the Gentest Corporation. This was derived from the original *CYP2D6*-Met cDNA isolated by Gonzalez et al. [12], expressed heterologously in human lymphoblastoid cells. The present study has shown that the catalytic activity and the stereoselectivity of CYP2D6-Met is similar, irrespective of whether microsomes containing CYP2D6-Met were derived from human lymphoblastoid or yeast cells (Table 3). Thus it would appear that there is fidelity in expression of the same cDNA across different host cells. In the case of CYP2D6-Met at least, differences in membrane composition (phospholipids and sterols) and NADPH cytochrome *P*-450 reductase (yeast or human) do not influence catalytic activity with respect to metoprolol oxidation. The recent availability of microsomes containing CYP2D6-Val derived from human lymphoblastoid cells (Gentest Corporation) will allow this claim to be examined further by comparison with yeast-derived CYP2D6-Val.

In conclusion, molecular modelling studies based on the alignment of CYP2D6 with CYP102 places amino acid residue 374 directly in the active site of the enzyme and in a position to influence the regioselective oxidation of metoprolol. However, the residue is sufficiently distant from the chiral centre of metoprolol so as not to influence the enantioselective metabolism of this substrate. These observations are in complete agreement with the experimental data. The modelling studies also corroborate the participation of aspartic acid-301 in the electrostatic interaction with the basic nitrogen of the substrate. Furthermore, the model proposes serine-304 as a determinant of CYP2D6 enantioselectivity, as observed with metoprolol and other β-blockers, through the ability of this amino acid residue to hydrogen bond with substrates.

This work was funded partly by the Wellcome Trust (038735). We gratefully acknowledge the expert technical assistance of J. R. Harlow (Sheffield), and G. Smith (Dundee) for helpful discussions.

REFERENCES

1 Eichelbaum, M. and Gross, A. S. (1990) Pharmacol. Ther. **46**, 377–394
2 Tucker, G. T. (1994) J. Pharm. Pharmacol. **46**, 417–424
3 Tucker, G. T., Lennard, M. S., Ellis, S. W., Woods, H. F., Cho, A. K., Lin, L. Y., Hiratsuka, A., Schmitz, D. A. and Chu, T. Y. Y. (1994) Biochem. Pharmacol. **47**, 1151–1156
4 Mahgoub, A., Idle, J. R., Dring, L. G., Lancaster, R. and Smith, R. L. (1977) Lancet **i**, 584–586
5 Tucker, G. T., Silas, J. H., Iyun, A. O., Lennard, M. S. and Smith, A. J. (1977) Lancet **ii**, 718
6 Eichelbaum, M., Spannbruker, N., Steincke, B. and Dengler, J. J. (1979) Eur. J. Clin. Pharmacol. **16**, 183–187
7 Gough, A. C., Miles, J. S., Spurr, N. K., Moss, J. E., Gaedigk, A., Eichelbaum, M. and Wolf, C. R. (1990) Nature (London) **347**, 773–776
8 Gonzalez, F. J. and Meyer, U. A. (1991) Clin. Pharmacol. Ther. **50**, 233–238
9 Broly, F., Gaedigk, A., Heim, M., Eichelbaum, M., Morike, K. and Meyer, U. A. (1991) DNA Cell Biol. **10**, 545–558
10 Saxena, R., Shaw, G. L., Relling, M. W., Frame, J. N., Moir, D. T., Evans, W. E., Caporaso, N. and Weiffenbach, B. (1994) Hum. Mol. Genet. **3**, 923–926
11 Evert, B., Griese, E.-U. and Eichelbaum, M. (1994) Naunyn-Schmiedeberg's Arch. Pharmacol. **350**, 434–439
12 Gonzalez, F. J., Skoda, R. C., Kimura, S., Umeno, M., Zanger, U., Nebert, D. W., Gelboin, H. V., Hardwick, J. P. and Meyer, U. A. (1988) Nature (London) **331**, 442–446
13 Kimura, S., Umeno, M., Skoda, R. C., Meyer, U. A. and Gonzalez, F. J. (1989) Am. J. Hum. Genet. **45**, 889–904
14 Ellis, S. W., Ching, M. S., Watson, P. F., Henderson, C. J., Simula, A. P., Lennard, M. S., Tucker, G. T. and Woods, H. F. (1992) Biochem. Pharmacol. **44**, 617–620
15 Ellis, S. W., Rowland, K., Harlow, J. R., Simula, A. P., Lennard, M. S., Woods, H. F., Tucker, G. T. and Wolf, C. R. (1994) Br. J. Pharmacol. **112**, 244P
16 Gotoh, O. (1992) J. Biol. Chem. **267**, 83–90
17 Korzekwa , K. R. and Jones, J. P. (1993) Pharmacogenetics **3**, 1–18
18 Lewis, D. F. V. (1995) Xenobiotica **25**, 333–366
19 Hasemann, C. A., Kurumbail, R. G., Boddupalli, S. S., Peterson, J. A. and Deisenhofer, J. (1995) Structure **3**, 41–62
20 Poulos, T. L., Finzel, B. C. and Howard, A. J. (1987) J. Mol. Biol. **195**, 687–700
21 Ravichandran, K. G., Boddupalli, S. S., Hasemann, C. A., Peterson, J. A. and Deisenhofer, J. (1993) Science **261**, 731–736
22 Hasemann, C. A., Ravichandran, K. G., Peterson, J. A. and Deisenhofer, J. (1994) J. Mol. Biol. **236**, 1169–1185
23 Koymans, L. M. H., Vermeulen, N. P. E., Baarslag, A. and Donne-Op den Kelder, G. M. (1993) J. Comput.-Aided Mol. Design **7**, 281–289
24 Otton, S. V., Crewe, H. K., Lennard, M. S., Tucker, G. T. and Woods, H. F. (1988) J. Pharmacol. Exp. Ther. **247**, 242–247
25 Williams, M. L., Lennard, M. S., Martin, I. J. and Tucker, G. T. (1994) Carcinogenesis **15**, 2733–2738
26 Sambrook, J., Fritsch, E. F. and Maniatis, T. (1989) Molecular Cloning, a Laboratory Manual. 2nd edn., Cold Spring Harbour Laboratory Press, Cold Spring Harbour
27 Becker, D. M. and Guarente, L. (1991) Methods Enzymol. **194**, 182–187
28 Shaw, L., Lennard, M. S., Tucker, G. T., Bax, N. D. S. and Woods, H. F. (1987) Biochem. Pharmacol. **36**, 2283–2288
29 Omura, T. and Sato, R. (1964) J. Biol. Chem. **239**, 2370–2378
30 Jefcoate, C. R. (1978) Methods Enzymol. **52**, 258–279
31 Bernstein, F. C., Koetzle, T. F., Williams, G. J. B., Meyer, E. F., Brice, M. D., Rodgers, J. R., Kennard, O., Shimanouchi, T. and Tasumi, M. (1977) J. Mol. Biol. **112**, 535–542
32 Weiner, S. J., Kollman, P. A., Case, D. A., Chandra Singh, U., Ghio, C., Alagona, G., Profeta, S., Jr. and Weiner, P. (1984) J. Amer. Chem. Soc. **106**, 765–784
33 Islam, S. A., Wolf, C. R., Lennard, M. S. and Sternberg, M. J. E. (1991) Carcinogenesis **12**, 2211–2219
34 Wolff, T., Distlerath, L. M., Worthington, M. T., Groopman, J. D., Hammons, G. J., Kadlubar, F. F., Prough, R. A., Martin, M. V. and Guengerich, F. P. (1985) Cancer Res. **45**, 2116–2122
35 Ellis, S. W., Hayhurst, G. P., Smith, G., Lightfoot, T., Wong, M. M. S., Simula, A. P., Ackland, M. J., Sternberg, M. J. E., Lennard, M. S., Tucker, G. T. and Wolf, C. R. (1995) J. Biol. Chem. **270**, 29055–29058
36 Meyer, U. A., Gut, J., Kronbach, T., Skoda, C., Meier, U. T. and Catin, T. (1986) Xenobiotica **16**, 449–464
37 Koymans, L. M. H., Vermeulen, N. P. E., Van Acker, S. A. B. E., Te Koppele, J. M., Heykants, J. J. P., Lavtijsen, K., Meuldermans, W. and Donne-Op den Kelder, G. M. (1992) Chem. Res. Toxicol. **5**, 211–219
38 Cupp-Vickery, J. R. and Poulos, T. L. (1995) Struc. Biol. **2**, 144–153
39 Ouzonis, C. A. and Melvin, W. T. (1991) Eur. J. Biochem. **198**, 307–315
40 Kim, M., Shen, D. D., Eddy, A. C. and Nelson, W. L. (1993) Drug Metab. Dispos. **21**, 309–317
41 Mautz, D. S., Nelson, W. L. and Shen, D. D. (1995) Drug Metab. Dispos. **23**, 513–517

Received 27 October 1995/22 December 1995; accepted 26 January 1996